Pure appl. geophys. 164 (2007) 975–998
0033–4553/07/050975–24
DOI 10.1007/s00024-007-0196-5

Pure and Applied Geophysics

Regional Geothermal Characterisation of East Anatolia from Aeromagnetic, Heat Flow and Gravity Data

Özcan Bektaş,[1,3] Dhananjay Ravat,[2] Aydin Büyüksaraç,[1] Funda Bilim,[1] and Abdullah Ateş[3]

Abstract—East Anatolia is a region of high topography made up of a 2-km high plateau and Neogene and Quaternary volcanics overlying the subduction-accretion complex formed by the process of collision. The aeromagnetic and gravity data surveyed by the Mineral Research and Exploration (MTA) of Turkey have been used to interpret qualitatively the characteristics of the near-surface geology of the region. The residual aeromagnetic data were low-pass filtered and analyzed to produce the estimates of magnetic bottom using the centroid method and by forward modelling of spectra to evaluate the uncertainties in such estimates. The magnetic bottom estimates can be indicative of temperatures in the crust because magnetic minerals lose their spontaneous magnetization at the Curie temperature of the dominant magnetic minerals in the rocks and, thus, also are called Curie point depths (CPDs). The Curie point depths over the region of Eastern Anatolia vary from 12.9 to 22.6 km. Depths computed from forward modelling of spectra with 200–600 km window sizes suggest that the bottom depths from East Anatolia from the magnetic data may have errors exceeding 5 km; however, most of the obtained depths appear to lie in the above range and indicate that the lower crust is either demagnetized or non-magnetic. In the interpretation of the magnetic map, we also used reduction-to-pole (RTP) and amplitude of total gradient of high-pass filtered anomalies, which reduced dipolar orientation effects of induced aeromagnetic anomalies. However, the features of the RTP and the total gradient of the high-pass filtered aeromagnetic anomalies are not highly correlated to the hot spring water locations. On the other hand, many high-amplitude features seen on the total gradient map can be correlated with the ophiolitic rocks observed on the surface. This interpretation is supported by Bouguer gravity data. In this paper, we recommend that the sources of the widespread thermal activity seen in East Anatolia must be investigated individually by means of detailed mapping and modelling of high resolution geophysical data to assess further the geothermal potential of the region.

Key words: Aeromagnetic anomalies, gravity data, power spectrum, curie point depth, forward modelling, upper crustal structure.

[1] Faculty of Engineering, Department of Geophysical Engineering, Cumhuriyet University, 58140, Sivas, Turkey. E-mail: absarac@cumhuriyet.edu.tr

[2] Department of Geology 4324, Southern Illinois University Carbondale, Carbondale, Illinois, 62901-4324, United States.

[3] Faculty of Engineering, Department of Geophysical Engineering, Ankara University, 06100, Besevler, Ankara, Turkey.

1. Introduction

Surface geology of East Anatolia is complex as a result of recent active tectonic and volcanic activity. The region is composed of major tectonic units of Pontides, Anatolid-Tauride belt and Bitlis suture zone, North and East Anatolian faults (BINGOL, 1989; KOCYIGIT *et al.,* 2001). In many parts of East Anatolia, ophiolitic and young volcanic rocks (of ages 3–12 Ma, KESKIN, 2003) can be observed (Fig. 1). The North and East Anatolian faults formed as a result of the compressional regime in the region (ZOR *et al.*, 2003). A recent analysis was made by STORETVEDT (2003) who suggested a new mobilistic theory of continental collision of the Eurasian and African plates. As a result of this collision, the Anatolian plate has been rotating counter-clockwise and moving westwards since ~5 Ma (MCCLUSKY *et al.*, 2000). Topography is very rugged in East Anatolia (Fig. 2) and there are several high mountains such as Ararat, Suphan and Nemrut.

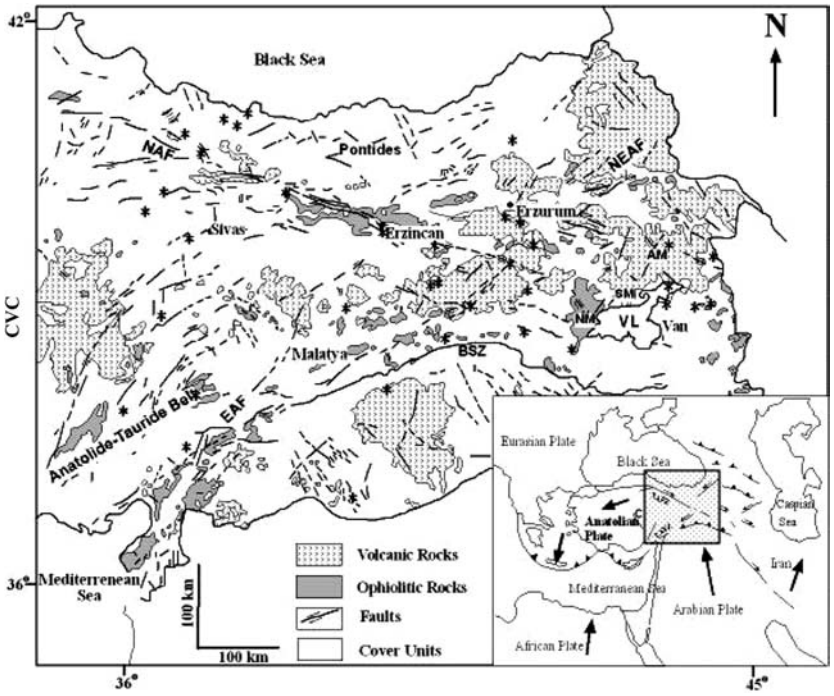

Figure 1
Geological map of East Anatolia (Simplified from BINGOL, 1989). Inset map shows the location of the study area. EAF: East Anatolian Fault, NAF: North Anatolian Fault, MF: Malatya Fault, VL: Van Lake, AM: Ararat Mountain, SM: Suphan Mountain, NM: Nemrut Mountain, BSZ: Bitlis Suture Zone, NEAF: North East Anatolian Fault, ATB: Anatolide-Tauride Belt. * shows hot spring locations. CVC: Cappadocia Volcanic Center. C sign in the inset map shows the location of Cappadocia.

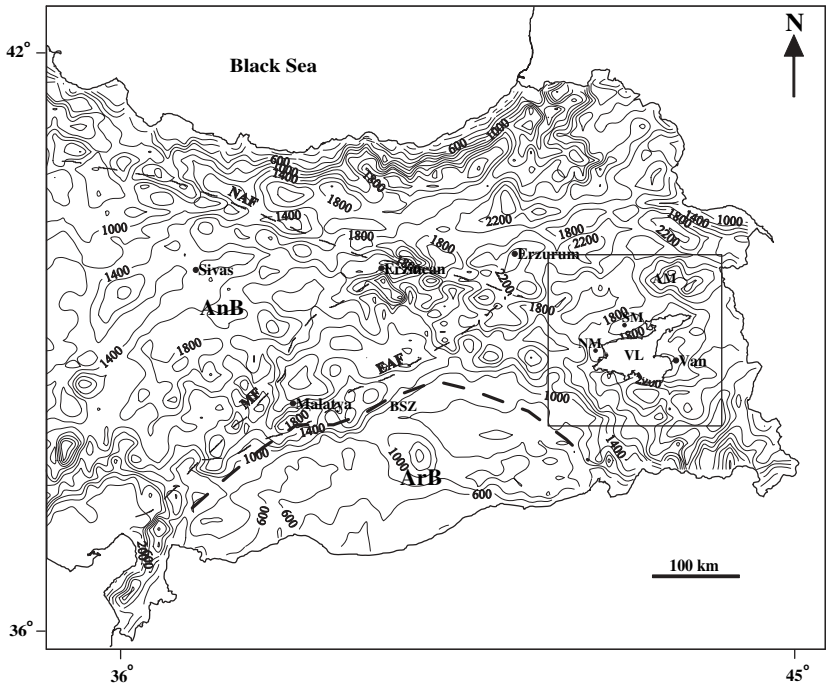

Figure 2
Topographic map of East Anatolia. Contour interval is 200 m. EAF: East Anatolian Fault, NAF: North Anatolian Fault, VL: Van Lake, BSZ: Bitlis Suture Zone, AM: Ararat Mountain, SM: Suphan Mountain, NM: Nemrut Mountain, AnB: Anatolian Block, ArB: Arabian Block. Black squared line shows high topographic and volcanic regions in East Anatolia. Locations of important cities are shown.

In tectonically young regions, surface heat flow can be dominated by the young, localized volcanic activity that may or may not have geothermal potential significance, depending on the age and the extent of hot rocks and the heat flow from the mantle. The surface heat flow is also affected by heat production in the crust. Lacking information on these parameters, one must make assumptions regarding the thickness of young volcanic units and knowledge of heat production in the crust. Some of this information can be inferred from seismic data and by modelling gravity and magnetic anomaly fields. In addition, there are several spectral methods useful in inferring the estimates of the bottom of the magnetic layer. Demagnetization caused by the Curie temperature phenomenon reflects temperatures in the crust at that depth, and magnetically sensed bottom estimates can be helpful in deriving this depth. Together, the information from surface heat flow and magnetically inferred temperatures in the crust could be useful in the exploration of geothermal energy and various tectonically important parameters.

Significant amounts of research and exploration have been carried out to understand the geothermal variation of Turkey. In a first comprehensive study, the

preparation of the heat flow map for the whole country was carried out by using temperature gradients in wells (TEZCAN, 1979; TEZCAN and TURGAY, 1987). ATES *et al.* (2003) computed the Curie depths according to the method of CONNARD *et al.* (1983) from the aeromagnetic anomalies of the Marmara Sea region, northwest Turkey. It was suggested that inferred thin crust in the region would play a key role for determining the cause of earthquakes in this seismically active region. ATES *et al.* (2005) studied Curie point depth of central Anatolia and found extremely shallow Curie depths around 8 km near Cappadocia in the western extremity of Figure 1. Their thermal gradient map exhibits high thermal gradient values from Ankara to Kayseri.

A recent Curie point depth map was published by AYDIN *et al.* (2005) demonstrating reasonable correlation in west and central Turkey with the previous work in the region (DOLMAZ *et al.*, 2005a, b; ATES *et al.*, 2005). However, the detailed variations inferred in their study and our results in this paper for Eastern Anatolia are different in many places. One reason for the difference is as follows: AYDIN *et al.* (2005) used the method of TANAKA *et al.* (1999), who modified the implementation of the method of BHATTACHARYYA and LEU (1975) and OKUBO *et al.* (1985) by attempting to justify the selection of slopes for the layer top and the layer centroid from different segments of the respective power spectra. RAVAT *et al.* (2005) found that this modification is difficult to implement in practice because different segments of the power spectra can be in reality associated with different magnetic layers. Thus, using slopes from different segments in the case of a multi-layer magnetic model of the crust will likely lead to incorrect depth to the top of the deepest layer (because in reality, it could be associated with a shallower one) and, consequently, the bottom depth, based on the depth to the top and the centroid, would also be in error. Moreover, the shallow Curie depth estimates of AYDIN *et al.* (2005) in mountainous volcanic areas of east Anatolia of 6–8 Ma (PEARCE *et al.,* 1990) between 36° 50'N–39° N latitudes and 38°E–43°E longitudes could be caused by a strong correlation between aeromagnetic anomalies and topography which may have biased the spectral slopes in the intermediate spectral range (in the wavenumber range from 0.05 to 0.1).

In this paper, to remove effects of topography, aeromagnetic anomalies were low-pass filtered. The Curie point depths were computed on the low-pass filtered aeromagnetic anomalies. To check the validity of the Curie point depths, depths were computed using different methods and different window sizes (OKUBO *et al.*, 1985, and the forward modelling of the power spectrum slopes and minimum depth to the bottom as proposed by RAVAT *et al.*, 2005). In validating the forward modelled results, precaution was taken to ensure that only those results are accepted where the autocorrelation function of the Fourier spectra was nearly circular, indicating that there are no significant anomaly trends in the computed window that might affect the results (as shown by SHUEY *et al.*, 1977 and verified by RAVAT *et al.*, 2005).

1.1. Regional Geophysical Background

Eastern Anatolia is rich in terms of thermal activity. The activity is associated with the volcanism of the region, which is thought to have been caused by the subduction of the Arabian plate under the Anatolian plate in the east and the westward escape of the latter plate initiated in Miocene during the Alpine orogeny (KOCYIGIT *et al.*, 2001). Central and northern parts of East Anatolia display high amplitude aeromagnetic anomalies. In the south, over the Arabian platform, subdued aeromagnetic anomalies are observed. The Bouguer anomalies show regional east-west trends associated with the process of obduction and have superimposed patterns that reflect the characteristics of important NW and NE trending faults (Fig. 3). In the central part of Eastern Anatolia, there are numerous Bouguer anomaly lows reaching over –100 mGal, indicating either thicker crust in the region or thickening of upper crustal lower density layers. In addition, a number of negative contour closures of the Bouguer anomalies can be correlated with the cover units of the geological map (Fig. 1).

GURBUZ *et al.* (2004) and ZOR *et al.* (2003) determined average crustal thickness of 45 km for Eastern Anatolia. The crust thickens from 42 km near the southern part

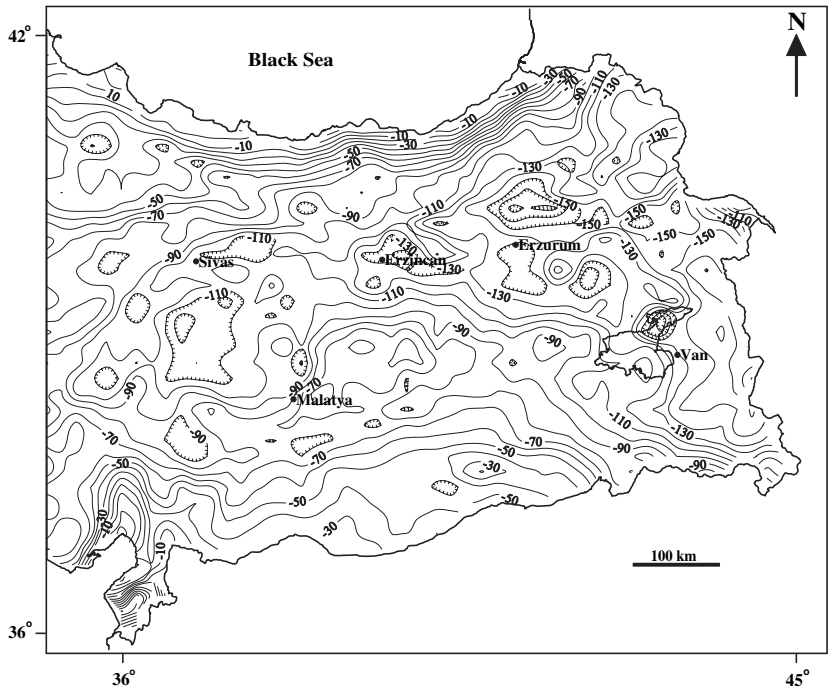

Figure 3
Bouguer anomaly map of East Anatolia. Contour interval is 10 mGal. Locations of important cities are shown. Lows are hachured.

of the Bitlis suture zone to 50 km along the North Anatolian Fault Zone (NAFZ) where Tethys was closed. In the east, crustal thickness increases from 40 km in the northern Arabian plate to 46–48 km in the middle of the Anatolian plateau. Based on seismicity, TURKELLI *et al.* (2003) suggested that the East Anatolian Fault Zone (EAFZ) and Bitlis suture zone's have thicker portions and more rigid crust than the NAFZ. AL-LAZKI *et al.* (2003) observed broad regional zones of low (< 8 km s^{-1}) and extremely low (< 7.8 km s^{-1}) short-wavelength Pn velocity anomalies beneath Northwestern Iran, Eastern Anatolian plateau, the Caucasus region and most of the Anatolian plate. They suggested that the very low Pn velocity is caused by the absence of lithospheric mantle in some parts of Eastern Anatolia.

2. The Aeromagnetic Data

The aeromagnetic data of East Anatolia were obtained from the General Directory of Mineral Exploration and Research Company (MTA) of Turkey. Flight lines vary between 1 and 5 km and the sampling along the flight lines is

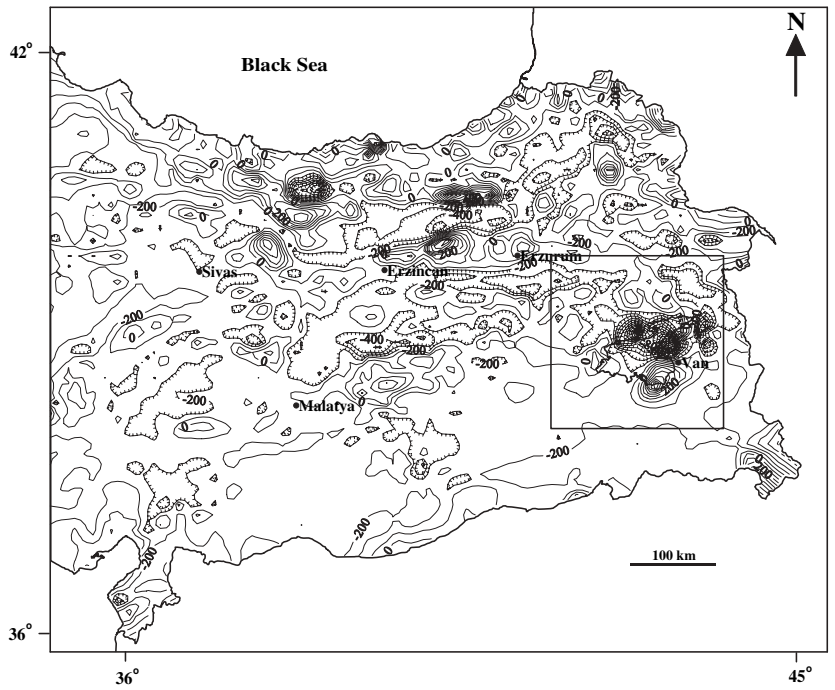

Figure 4
Residual total field aeromagnetic anomaly map of East Anatolia. Contour interval is 100 nT. Locations of important cities are shown. Lows are hachured.

approximately 70 m spacing at a mean terrain clearance of 600 m. All necessary corrections to the flight data were carried out by MTA, excluding the International Geomagnetic Reference Field (IGRF) correction. The original data are in the format of X (easting, m), Y (northing, m), Z (nT). MTA made available only the data gridded at 5 km interval (Fig. 4). The IGRF correction was done to the gridded data supplied by the MTA utilizing BALDWIN and LANGEL's (1993) algorithm. The residual total magnetic intensity map contoured at 75 nT intervals after the removal of the IGRF. The residual aeromagnetic anomalies shown in Figure 4 appear to be sufficiently isolated from the regional field implying that the IGRF calculation adequately represents the core dipole field and other regional magnetic anomaly fields. The high frequency magnetic anomalies near Van, Erzincan, east of Sivas and the northeast part of the study area appear to be associated with volcanic and ophiolitic rocks. Topographically higher regions appear to be correlated with the aeromagnetic anomalies because of the magnetic nature of the volcanic rocks at the surface. The topographic height increases from west to east as the crust becomes thicker in East Anatolia.

3. The Curie Point Depth of East Anatolia

Two of the earliest methods to calculate depths from aeromagnetic anomalies were published by SPECTOR and GRANT (1970) and BHATTACHARYYA and LEU (1975). One of the methods in this paper used to estimate the Curie point depths is the method based on the latter paper, reassessed by OKUBO *et al.* (1985). OKUBO *et al.* (1985, 1989) suggest that their method has an advantage that large dimensions of windows are not necessary to obtain the Curie point estimate; however, this is not found to be true in the experimentation performed by RAVAT *et al.* (2005) and also the results of CHIOZZI *et al.* (2005). Other limitations of the method are discussed later in the section.

The residual aeromagnetic anomalies were low-pass filtered at a cut-off wavenumber of 0.096 Km^{-1} to remove the effect of topography because we did not want to make errors in our depth estimates by inadvertently fitting the slopes to the power spectra of the shallow layers. The cut-off wavenumber was selected based on the changeover of the short-wavenumber and long-wavenumber segments of the azimuthally averaged power spectra of the entire region (Fig. 5).

Figure 6 shows the low-pass filtered aeromagnetic anomaly map. The low-pass filtered aeromagnetic anomalies do not appear to be correlated with topography and reflect anomalies of the deep-seated magnetized bodies.

The effect of highly magnetic volcanic rocks in the mountainous regions may have biased estimates from the AYDIN *et al.* (2005)'s study. We calculated spectral slopes from unfiltered and low-pass filtered anomalies to see the effects of topography and volcanic rocks. As an example, one can observe that the low

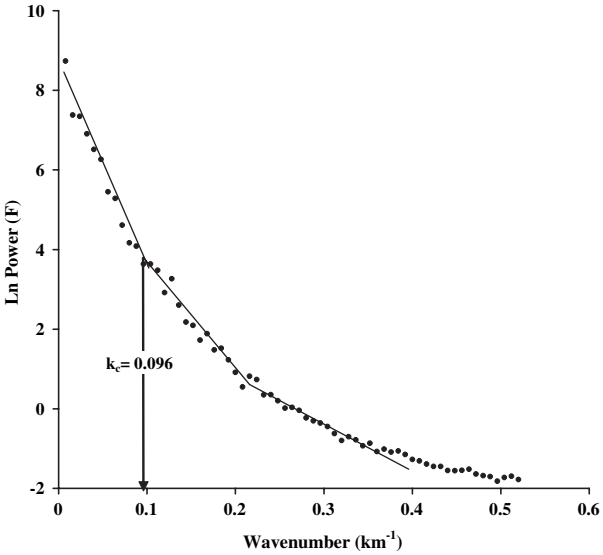

Figure 5
Power spectrum depth estimate Ln Power (F) versus wavenumber (km^{-1}) of the region shown in Figure 4 and arrow shows the cut-off frequency, $k_c = 0.096$ km^{-1} for low and high-pass filtering.

wavenumber character of the unfiltered and filtered spectra are quite different (Figs. 7a and 7b, respectively); the filtered spectra are consistent with the power law behavior expected from layered magnetization. Consequently, the depths to the top of the deepest sources from unfiltered and filtered data are 8.9 and 12.2 km, respectively. It appears that the unfiltered depth estimates, as computed by AYDIN *et al.* (2005), could be biased due to the long-wavelength effect of magnetic sources of topography.

Our results using large window sizes from 200 to 600 km suggested that spectral peaks are not observed over this region and therefore the region represents a layered magnetization situation. In our analysis we employed the centroid method of BHATTACHARYYA and LEU (1975) and OKUBO *et al.* (1985) with a 150-km window size to obtain our overall results and the depth to the top and the minimum depth to the centroid and the bottom using forward modelling of spectra (RAVAT *et al.*, 2005) to explore the uncertainty with window sizes of 200 to 600 km. This method was based on earlier simultaneous proposals of RAVAT (2004), FINN and RAVAT (2004) and ROSS *et al.* (2004).

The low-pass filtered aeromagnetic anomaly map was subdivided into 78 blocks of 150×150 km^2. All of the blocks overlap with each other by 75 km (Fig. 6). The bottom of the inferred magnetic bottom z_b can only be estimated if, z_o, the centroid can be accurately determined. In this method, the depth to the top (z_t) is derived from the smallest wavenumber straight slope segment of the azimuthally averaged power

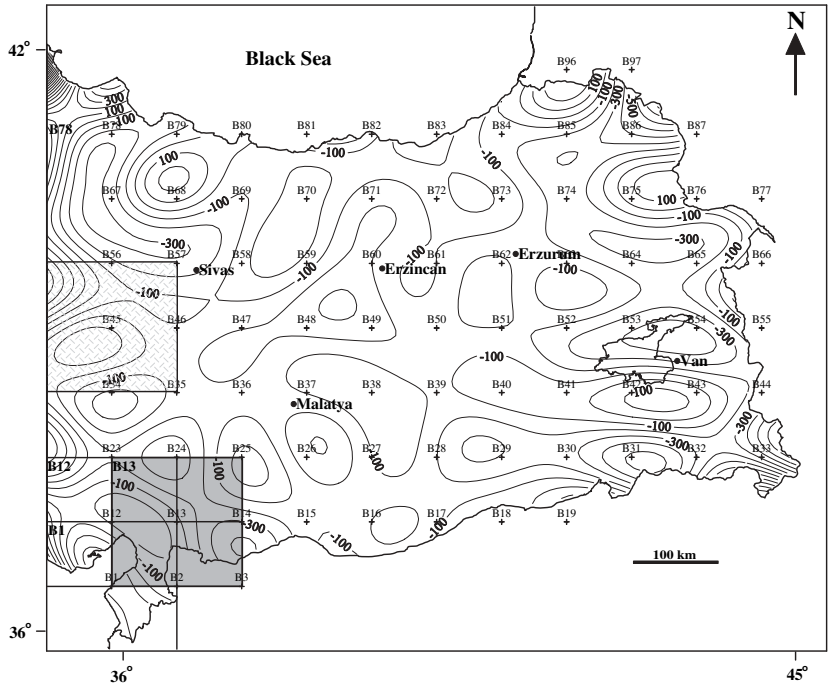

Figure 6
Low-pass filtered residual magnetic anomaly map of East Anatolia. Contour interval is 100 nT. The squares show selected three sample blocks, B1, B12 and B13. Block sizes are 150 × 150 km^2. + signs indicate centers of the blocks and numbers used for the Curie-point depth regions. Patterned square with number B45 shows power spectrum applied region in Figure 8. Locations of important cities are shown.

spectrum (SPECTOR and GRANT, 1970) (Fig. 8a). For the centroid of ensemble of rectangular prisms, OKUBO *et al.* (1985) used a power spectrum of the prism in the following form,

$$F(s,\psi) = 4\pi^2 VJ_s[N + i(L\cos\psi + M\sin\psi)] \times [n + i(l\cos\psi + m\sin\psi)] \times \exp[-2\pi is(x_0\cos\psi + y_0\sin\psi)] \times \exp(-2\pi sz_0), \quad (1)$$

where J = magnetization per unit volume, V = average body volume, L, M, N = direction cosines of the geomagnetic field, l, m, n = direction cosines of the average magnetization vector, x_0 and y_0 = average body x and y centre locations, $s = (u^2+v^2)^{1/2}$ and $\psi = \tan^{-1}(u/v)$ are polar wave number coordinates (not circular wavenumber, but equivalent to frequency, i.e., 1/distance unit). u and v are wavenumbers in x and y directions. The centroid depth, z_o, can be estimated, in a manner similar to the estimation of the depth to the top, from the frequency-scaled power spectra as (Fig. 8b)

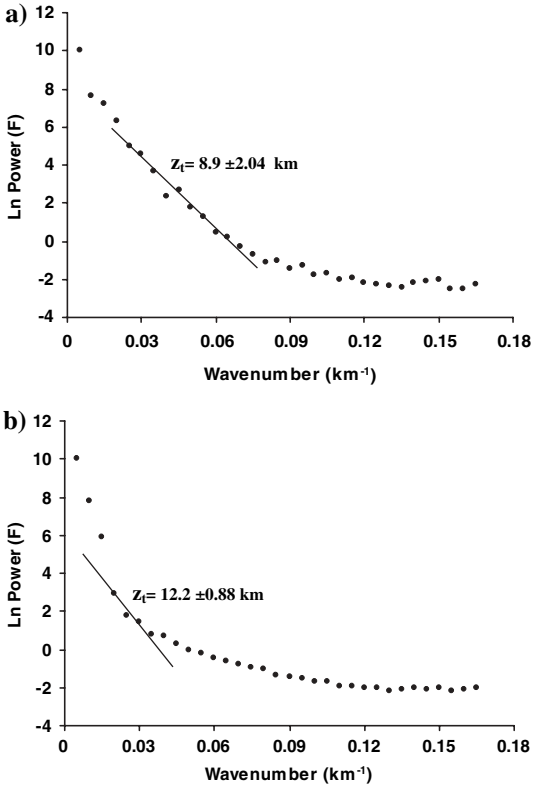

Figure 7
a) Power spectrum depth estimate Ln Power (F) versus wavenumber (km^{-1}) of the black squared line shown in Figure 4. b) Power spectrum depth estimate applied to the low-pass filtered anomalies shown in Figure 6.

$$G(s,\psi) = \frac{1}{s}F(s,\psi) \tag{2}$$

Finally, the depth of the Curie point is calculated by equation (3).

$$z_b = 2z_0 - z_t \tag{3}$$

where z_t and z_b are average depths to the top and bottom of the bodies and z_o is the depth to the centroid. The method was applied to all the blocks shown in Figure 6 and the slopes were determined using the method of least-squares. Calculated depth estimates for each of the 78 blocks were used to construct the magnetic bottom depth map (Fig. 9) at a contour interval of 1.0 km.

In addition to the centroid method, we have estimated the depths to the top and the minimum depth to the bottom of the deepest magnetic layer by forward modelling of the spectra using the following equation as recommended by RAVAT *et al.* (2005),

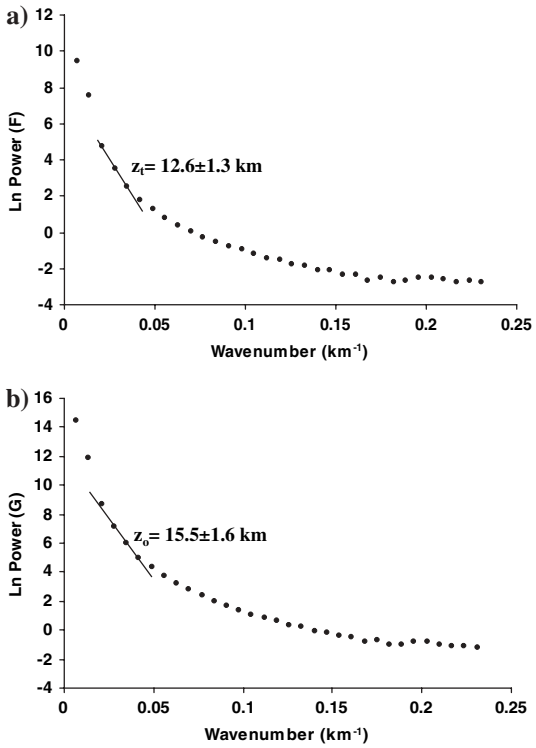

Figure 8
Spectral analysis for block number B45 for the low-pass filtered residual magnetic anomaly map (Fig. 6). a) Spectra calculated from $F(s,\psi)$ to estimate depth to z_t. Spectral analysis showing spectral peak for block number B45 for the low-pass filtered residual magnetic anomaly map (Fig. 6). Line shows the least-squares fit of the power spectra with standard deviations. b) Spectra calculated from $G(s,\psi)$ to estimate depth to centroid, z_o. Line shows the least-squares fit of the power spectra with standard deviations.

$$|F(k)|^2 = C\left(e^{-|k|z_t} - e^{-|k|z_b}\right)^2 \tag{4}$$

where $F(k)$ is the Fourier power spectrum, k is the wavenumber in cycles/km or 2π/km, and z_t and z_b are the depths to the top and bottom of magnetic sources. Constant C can be adjusted to move the modelled curve up or down to fit the slope. Because in this study the observed spectra showed no peaks and suggested layered magnetization due to their power-law appearance, the best we could do with this method in this situation is assess the uncertainty in the depth to the top and the "minimum" depth to the bottom of the layer that does not violate the observed power spectrum. Figure 10 depicts the example of a 300-km window in the study area where we see the modelled depth to the top yielding the high wavenumber slope of the spectra and the modelled depth to the bottom yielding the shape of the peak. The choice of a shallower depth to the bottom will move the peak to the right and cross the observed spectra (which is not

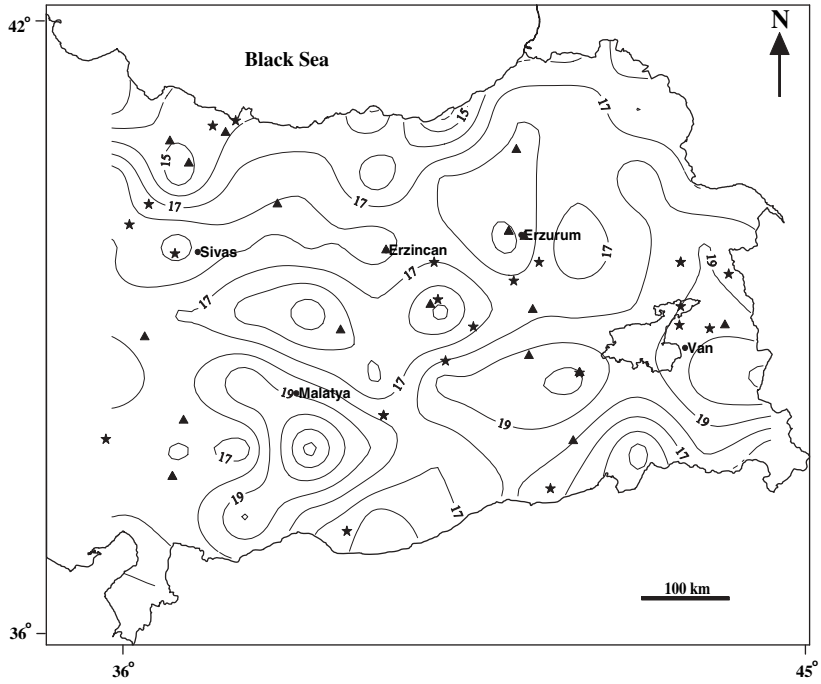

Figure 9
The estimated Curie point depths map from the low-pass filtered residual magnetic anomaly data. Contour interval is 1 km. ★: Hot springs with greater than 45°C temperatures ▲: Hot springs with less than 45°C temperatures. Locations of important cities are shown.

acceptable), whereas a deeper depth to bottom will move the peak to the left (this does not violate the observed spectra). Thus, if the estimate is chosen such that the computed spectra is as far to the right without crossing the observed spectra, the derived estimate is a minimum estimate of the depth to the bottom. We have ascertained that fitting a power law instead of the above equation does not yield meaningful depths to the bottom because of non-uniqueness between the power law exponent of crustal magnetization and the depth extent of the magnetized layer.

To assess the uncertainties in the derived CPDs, we used the above forward modelling method and computed depths with different window sizes from 200 to 600 km multiple times. We used only window locations away from the edges and where the autocorrelation function of the power spectrum was nearly circular. The presence of trends and regional effects in the data causes oblong trends and the non-circular shape of the autocorrelation of the power spectrum and makes the azimuthally averaged power spectrum unsuitable for the depth analysis (SHUEY *et al.*, 1977). The results showed that the estimates of the depth to the bottom were non-unique with the minimum uncertainty of 5 km. The calculated minimum depth ranges for 200 km windows vary from 11 to 13 kms around Sivas, near Erzincan they

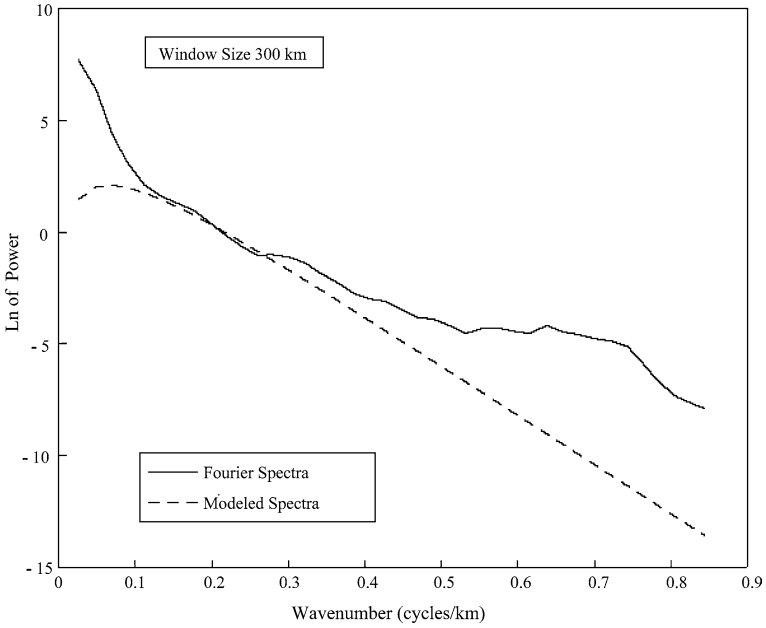

Figure 10
An example of the forward modelling of spectra using equation (4). The continuous line is the observed Fourier spectra for a 300 km window. In this case, OKUBO *et al.* (1985) method yielded depths of ~9.5 km for the depth to the top of the deepest layer and 14–15 km for the depth to the bottom. The forward modelling led to 10 km as the depth to the top of the deepest layer and 20 km as the minimum depth to the bottom. See text for other details about the usage.

are deeper around 20–22 km, but near Van Lake they are highly variable (18–29 km) between different runs (see Fig. 1 for locations). The calculated minimum depth range for 300 km windows is 13–15 km around north of Malatya, although once again highly variable west of Van Lake. Representative results of calculated minimum depths for 400, 500 and 600 km window sized range from 15 to 30 km in the map area. Because of differences in spatial variation of the estimates from one run to another (which arise from the differences in slope segments chosen from one run to the next), it is difficult to believe that the spatial variability is meaningful. On the other hand, many minimum magnetic bottom depths' determinations in the region yield the depths closer to 20 km.

In Kars, Agri and Van region the Curie point depth of AYDIN *et al.* (2005) is as shallow as 6 km. In this region, our Curie point depth map (Fig. 9), based on the low-pass filtered aeromagnetic anomalies, shows much deeper Curie depth level (>17 km). Around Malatya and Bingol towns along E-W direction due to the overlapping percentage of 50% and magnetic anomalies trending in E-W direction, the Curie point depth map of AYDIN *et al.* (2005) displays similarly shallow Curie levels, which are certainly caused by the high topography as explained. We further

investigate the validity of the derived approximate 20 km Curie depth by considering the probable magnetic mineralogies and the lithospheric geotherms for the region.

4. Discussion

The crust of Eastern Anatolia can be divided in several segments associated with two subduction episodes; one in the north near Pontides domain and another near the Bitlis suture (KESKIN, 2003). Near the Black Sea, the volcanic arc of Pontides with its accreted 50-km thick crust with calc-alkaline volcanic products (~11 Ma) dominates (KESKIN *et al.*, 1998), whereas in the central section much of the 45-km thick crust is likely to be made up of accretionary prism of mostly sediments and some scraped up oceanic basalts intruded by 11–6 Ma. Volcanism and plutonism of mixed calc-alkaline to alkaline nature (PEARCE *et al.*, 1990) have a suite of mafic to silicic components (KESKIN, 2003); the rocks of silicic components in this suite should have magnetite dominated mineralogies. Another complexity here is that constituents of much of the accretionary prism may be non-magnetic and the magnetic bottom for this case could have reflected the bottom of the intruded plutonic units and not the Curie depths. However, the volcanism is young (11–6 Ma) and the bottom portions of the plutonic middle crust at some 20-km depth may still be above the Curie temperatures of the magnetic minerals (e.g., magnetite) in the region. In the southern parts, younger and once again supracrustal mafic and silicic rocks probably rooted in their equivalent plutonic rocks are present (ERCAN *et al.*, 1990; PEARCE *et al.*, 1990). Thus, from the Black Sea up to the domain of the Bitlis-Pötürge zone, the rocks are likely to be dominated from more magnetite-bearing mineralogies with the Curie temperature of 580°C. The Bitlis-Poturge zone is dominated by metamorphic products and it is difficult to determine dominant magnetic materials in the zone without specific studies.

However, the contours of the magnetic bottom depths do not appear to be correlated with the suture zone. The region south of the Bitlis suture is cratonic and associated with the Arabian lithosphere. It is possible that the rocks in this domain are felsic in the upper crust and mafic in the lower crust as most commonly inferred in cratons. In the central part of the Arabian domain, where there is very young (<1 Ma) alkaline – primarily basaltic – intra-plate volcanism (KESKIN, 2003), titanomagnetite dominated magnetic mineralogies (with Curie temperatures of 300°–500°C) might predominate. Thus, in much of the central and northern parts of Eastern Anatolia and the parts of the Arabian domain, magnetite dominated Curie temperature of about 580°C may be justified. In the central parts of the Arabian domain, the temperatures might be more consistent with the Curie point of titanomagneties (i.e., lower than 580°C). The strongest correlation of the magnetically derived depths and geology appears to be with the expansive volcanic units in the west-central Eastern Anatolia and the gradient along the NAF in the west. It

Table 1

The locations and thermal degrees of hot springs in East Anatolia. ★ sign shows hot springs with water temperature greater than 45°C, ▲ sign shows hot springs with water temperature less than 45°C (ERISEN et al., 1996). Some locations are very close to each other with different thermal degrees. Thus, these are printed in bold type

Hot Spring Location Name	Location		Temperature (°C)	Symbols
	Latitude (North)	Longitude (East)		
Diyadin	**39°38′**	**43°22′**	**34–71**	★
Koprucermik	**39°38′**	**43°22′**	**34–71**	★
Yilanli	39°31′	44°00′	34–71	★
Kos	39°00′	40°38′	36–47	★
Haciyan	38°40′	40°16′	62	★
Harur	39°16′	40°10′	52	★
Hozavit	39°38′	40°07′	48	★
Haskoy	39°13′	40°04′	32–32.5	★
Nemrut	**38°33′**	**42°02′**	**18–66**	★
Ilicakoy	**38°33′**	**42°02′**	**44**	▲
Guroymak	**38°33′**	**42°02′**	**37.5–39**	▲
Cermik–1	**38°08′**	**39°27′**	**48**	★
Cermik–2	**38°08′**	**39°27′**	**51**	★
Kolan	38°58′	38°53′	42	▲
Bogert–Eksisu	39°45′	39°29′	31	▲
Ilica	**39°56′**	**41°06′**	**39**	▲
Ilica–2	**39°56′**	**41°06′**	**39**	▲
Pasinler	39°38′	41°31′	30–41	▲
Kigihamzan	39°27′	41°10′	56	★
Tekman–Yigitler	39°38′	41°30′	33–56	★
Ciftgoz	**38°54′**	**35°05′**	**34.5**	▲
Tekgoz	**38°54′**	**35°05′**	**41**	▲
Selale	**38°54′**	**35°05′**	**30**	▲
Bayramhaci	38°47′	35°01′	40	▲
Suleymanli	38°05′	36°49′	39.9–44	▲
Hartlap	**37°32′**	**36°40′**	**32–37**	▲
Yeldegirmeni	**37°32′**	**36°40′**	**30–36**	▲
Germiab	37°25′	41°39′	61	★
Yukarialagoz	39°10′	41°25′	30	▲
Bazikan	38°43′	41°22′	38	▲
Fatsa–Saramasik	41°01′	37°30′	48	★
Ayder	40°44′	41°12′	33–47	▲
Havza	40°58′	35°39′	51–54	★
Ladik–Hamamayagi	40°54′	35°53′	36–38	▲
Billoris	37°53′	41°57′	38	▲
Sicakcermik	39°43′	36°42′	36–50	★
Akcaagil	40°12′	38°03′	43	▲
Resadiye	40°12′	35°42′	50–55	★
Sulusaray	40°00′	36°06′	50–54	★
Erbaa–Gokbel	40°49′	36°38′	40.5	▲
Sariyazi	40°36′	36°53′	32	▲
Yardimci–Karaali	37°00′	38°58′	48	★
Hasanabdal	39°12′	43°22′	63–68	★
Zilan	39°01′	43°21′	90	★

Table 1

(Contd.)

Hot Spring Location Name	Location		Temperature (°C)	Symbols
	Latitude (North)	Longitude (East)		
Ayranci	38°59′	43°45′	47	★
Bugulu	39°01′	43°57′	37	▲
Bogazliyan–Cavlak	39°11′	35°14′	34–40.5	▲
Bogazliyan–Uzunlu	39°15′	35°23′	30	▲
Akdagmagdeni	39°39′	35°53′	30–39	▲
Sorgun	39°48′	35°11′	50–61	★
Sarikaya	39°29′	35°22′	46.5–48	★

appears that the volcanic units in the west have thicker plutonic roots and thus the Curie depths there reach around 18 km. Along the NAF in the west, the Curie depths are shallow (up to 15 km); the higher temperatures in the crust here are consistent with the presence of hot springs in the region (Table 1).

In the previous section we suggested, based on the discordance between the magnetic bottom depth estimates among different runs, different window sizes, and different methods, that the most reasonable interpretation we can make regarding the magnetic bottom depth is approximately 20 ± 5 km. We further inferred in this section that in most places in Eastern Anatolia the magnetic mineralogy is likely to be dominated by magnetite with *Tc* of 580°C. In a classic paper, LACHENBRUCH and SASS (1978) have modelled steady-state geotherms under a variety of circumstances such as extension, magmatic underplating, and intrusion. Using their formulation, we have attempted to understand the parameters for which the surface heat flow and Curie depth conditions in East Anatolia can be matched for steady-state conditions with and without intrusions in the crust. We assume thermal conductivity of 2.5 $Wm^{-1}K^{-1}$ and a 10-km thick upper layer with heat production of 2.09 $\mu W\ m^{-3}$ and vary asthenospheric heat flow (qa), lithospheric thickness (whose bottom is defined by the solidus temperature by the depth (pressure) dependent relationship, $T(z) = 1050°C + 3°C/km * z$ and the strain rate in % $(m.y.)^{-1}$ which suggests how intruded the crust can be. We derived two models, one with and one without intrusions, which yielded surface heat flow (qs) of about 90 mWm^{-2} – a value observed in many locations in East Anatolia (TEZCAN and TURGAY, 1989) and roughly 600°C at the depth of about 20 ± 5 km in the crust. Such values can be found for lithospheric thickness of 40 km in the case of a model without intrusion when the asthenospheric heat flow (qa) is 68 mW m^{-2} (Fig. 11a) and around 53 km for the intrusion model with a strain rate of 0.75 % $(m.y)^{-1}$ when the asthenospheric heat flow (qa) is 42 mW m^{-2} (Fig. 11b). It is important to note that observed variation in the values of heat production can lead to large variations in the obtained geotherms.

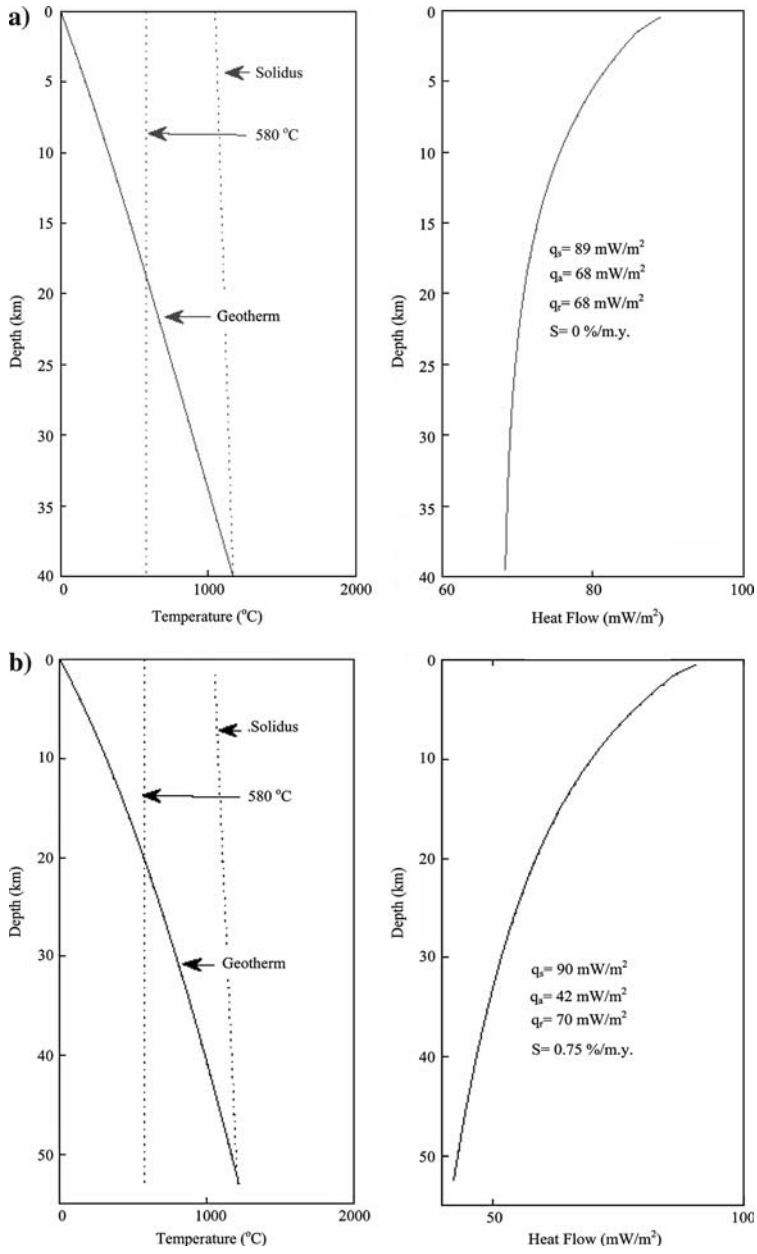

Figure 11

Steady-state geotherms (left panels) and heat flow with depth (right panels) computed using the methods of LACHENBRUCH and SASS (1978) to approximate the estimated conditions in the study area (see the text for details). a) Geotherm for the static case (where asthenospheric and reduced heat flow equal, i.e., $qa = qr$); and b) Geotherm with intrusion model with the strain rate of 0.75% $(my)^{-1}$.

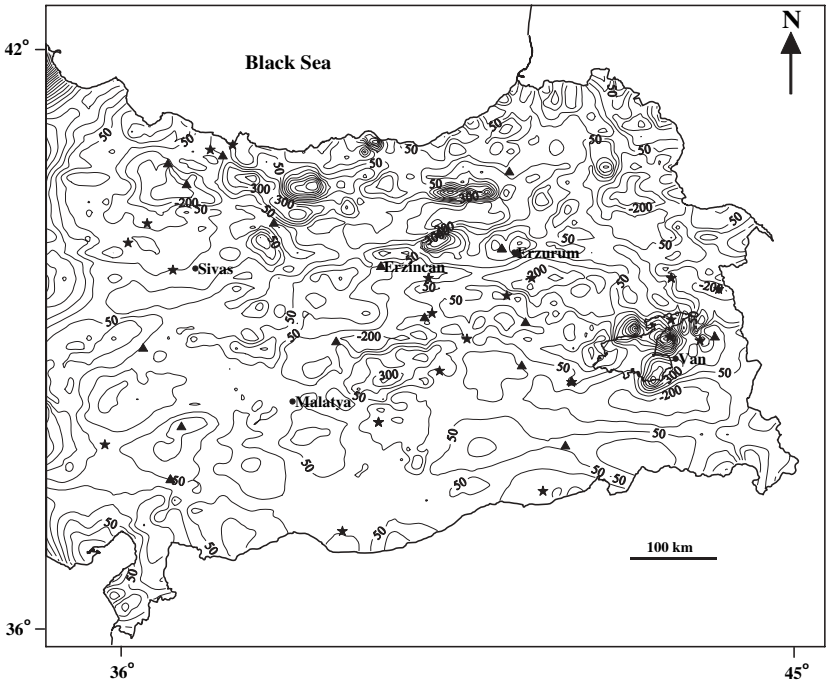

Figure 12
High-pass filtered aeromagnetic anomalies. Cut-off frequency is 0.096 Km^{-1}. Contour interval is 125 nT. ★, ▲ signs show hot springs with water temperature greater and less than 45°C, respectively. Locations of important cities are shown.

If we also take into account the fact that recent intrusive activity is widespread in East Anatolia, the intrusion model suggests that the lithosphere has thinned to at least 50–55 km and has led to the intrusive activity in the amount caused by the strain rate of 0.75% $(m.y)^{-1}$ (Fig. 11b). These values of lithospheric thickness are consistent with seismological observations of the crust and lithosphere thickness in the region. ZOR *et al.* (2003) and GURBUZ *et al.* (2004) determined an average crustal thickness of 45 km for Eastern Anatolia. The crust thickens from 42 km near the southern part of the Bitlis suture zone to 50 km along the North Anatolian Fault Zone (NAFZ) where Tethys was closed. In the east, crustal thickness increases from 40 km in the northern Arabian plate to 46–48 km in the middle of the Anatolian plateau. Based on seismicity, TURKELLI *et al.* (2003) suggested that the East Anatolian Fault Zone (EAFZ) and Bitlis suture zone have thicker portions and more rigid crust than the NAFZ. AL-LAZKI *et al.* (2003) observed broad regional zones of low (< 8 km s^{-1}) and extremely low (< 7.8 km s^{-1}) short-wavelength Pn velocity anomalies beneath Northwestern Iran, Eastern Anatolian plateau, the Caucasus region and most of the Anatolian plate. They suggested that

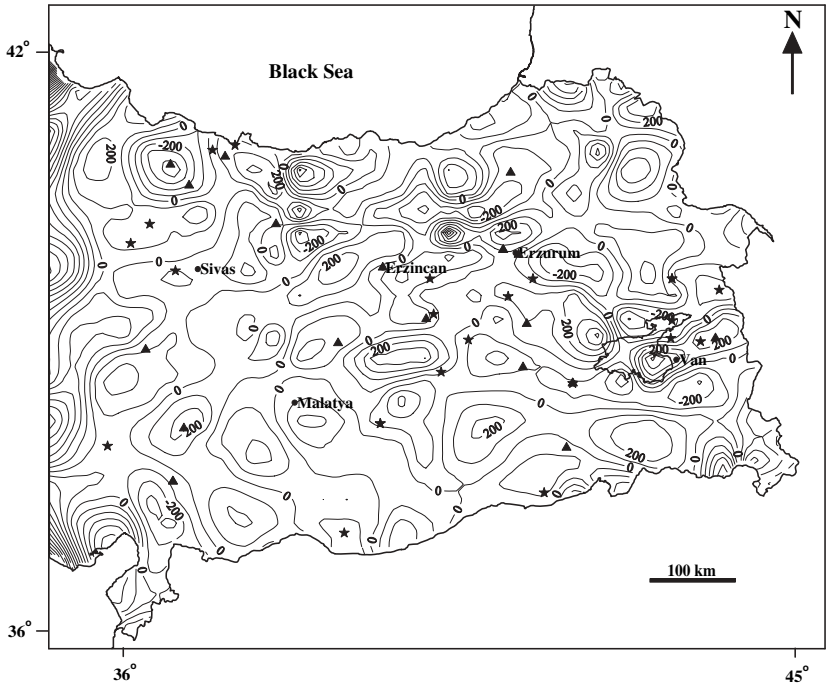

Figure 13
Reduction to pole transformation (RTP) of high-pass filtered aeromagnetic anomalies. Contour interval is 100 nT. ★: Hot springs with greater than 45°C temperatures ▲: Hot springs with less than 45°C temperatures. Locations of important cities are shown.

the very low Pn velocity is caused by the absence of lithospheric mantle in certain parts of Eastern Anatolia.

A lithospheric delamination which is one of the models proposed for the plateau uplift in East Anatolia (KESKIN, 2003) implies a rapid temperature change at the location of delamination.

In order to better understand the origin of observed magnetic variations in the regions, we have done additional analyses. For example, high-pass filtering enhances the shallow component of aeromagnetic anomalies. We chose the cut-off frequency, 0.096 km^{-1}, which was estimated from Figure 5, to derive the high-pass filtered aeromagnetic anomalies. The high-pass filtered aeromagnetic anomalies (Fig. 12) appear to be complex, due partly to dipolar effects caused by induced and remanent magnetization directions.

Reduction-to-pole transformation (RTP), which removes the skewness caused by the Earth's magnetic field (BLAKELY, 1995), was applied to the high-pass filtered residual aeromagnetic anomalies (Fig. 12) using the local field inclination. Because many of the anomalies are caused by the remanently magnetised near-surface volcanics (due to different remanent declination caused by the anticlockwise rotation

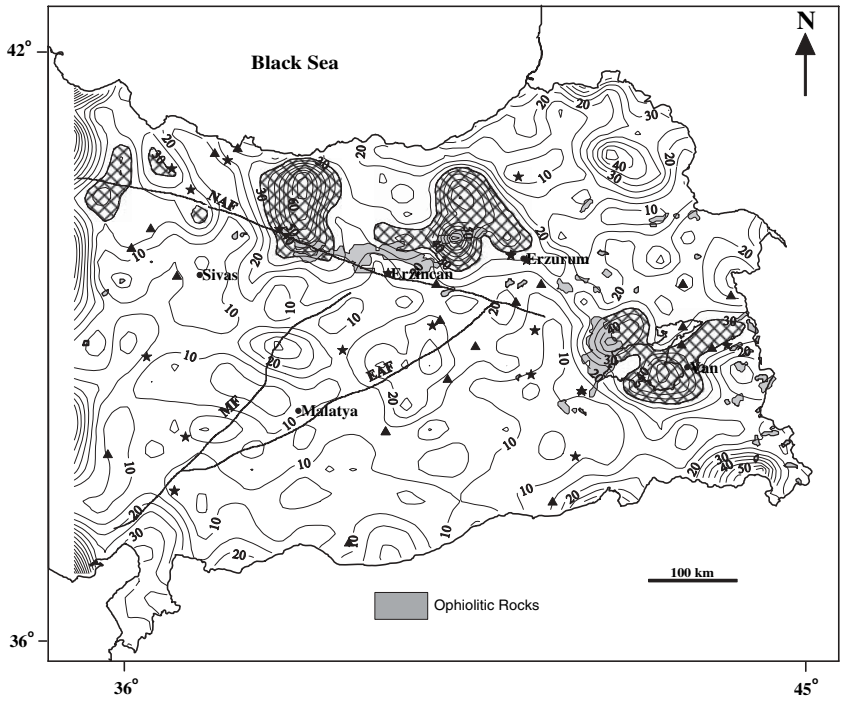

Figure 14
Amplitude of total gradient transformation of high-pass filtered aeromagnetic anomalies. Contour interval is 5 nT/m. ★: Hot springs with greater than 45°C temperatures ▲: Hot springs with less than 45°C temperatures. EAF: East Anatolian Fault, NAF: North Anatolian Fault, MF: Malatya Fault. The annotated places show high amplitude anomalies. Locations of important cities are shown.

of East Anatolia even though the volcanics are young and have remanent inclinations similar to the present-day field), most of the skewed anomalies were not corrected by the RTP transformation (Fig. 13). For strong remanent magnetization, the RTP map contains dipolar effects like those northeast of Erzurum, west of Van and west of Erzincan. In order to reduce the effect of the remaining remanent magnetization, a method known to reduce the effect of remanence in the anomaly field, the method of total gradient (ROEST *et al.*, 1992; BLAKELY, 1995) was applied to the high-pass filtered aeromagnetic anomalies. The amplitude function of the total gradient (ROEST *et al.*, 1992) is,

$$|A(x,y)| = \sqrt{\left(\frac{\partial M}{\partial x}\right)^2 + \left(\frac{\partial M}{\partial y}\right)^2 + \left(\frac{\partial M}{\partial z}\right)^2}. \quad (5)$$

Total gradient map of the short-wavelength components (Fig. 14) allows us to identify and map the near-surface volcanics somewhat more readily (even though the 3-D total gradient amplitude transformation – as opposed to 2-D transformation –

does not fully correct the effect of nonvertical magnetization in a nonvertical field) and take them into account in the overall interpretation.

High-amplitude total gradient anomalies observed in the north close to the shore of the Black Sea extending through north of Erzincan and west of Van Lake appear to be correlated with the ophiolitic rocks seen in the surface geology map (Fig. 1). These high-amplitude total gradient field anomalies are not correlated with the locations of the hot springs and volcanic formations. The Bouguer anomaly map (Fig. 3) also does not show positive anomalies over the ophiolitic rocks, affirming the interpretation that the strong magnetic features are related to ophiolites which have high magnetization, but low bulk density due to serpentinization (HESS, 1962) consistent with upper crustal lithologies. The long-wavelength gravity anomalies are consistent with the crustal thickness variations. The crustal thickness varies only a few km from its average values of 45–50 km in Eastern Anatolia (from the seismological work of PASYANOS *et al.*, 2004). It varies from 42 km near the southern part of the Bitlis suture zone to 50 km along North Anatolian fault, and increases from 40 km in the northern Arabian plate to 46–48 km in the middle of the Anatolian plateau (ZOR *et al.*, 2003). In addition, the Bouguer anomaly map illustrates trends associated with the North Anatolian fault and the Bitlis suture and has lows in this region that are consistent with the thickening of low density units expected in the compressional regime.

5. Conclusions

Curie point depth map of Eastern Anatolia, constructed from a spectral interpretation of magnetic anomaly data, shows that the magnetic thickness of the region varies from 13 to 23 km. For much of this region we are able to ascribe magnetite dominated magnetic mineralogy with the Curie point of 580°C; this suggests that the 580°C isotherm varies roughly from 13 to 23 km depth in the crust, implying that the temperatures are high within the crust in most locations. The anomalously high temperatures in the crust are also reflected in the high temperatures of hot springs (>45 °C) and in the young ages of volcanics in the region. It appears, however, that the high conductive mantle heat flow in the region may not have made it to the surface. Based on the analysis of magnetic and gravity anomaly maps and geology, it seems likely that the hot springs are tapping small upper crustal magma chambers and perhaps, in the regions of shallow CPDs (<17 km), hot near-surface plutons. It can be suggested therefore that the focus of geothermal resource evaluation and geophysical exploration should be on finding the heat sources of these hot springs, especially in the regions where the Curie depths shallower than 20 km are observed. Some of the major high-wavenumber magnetic anomalies are also clearly associated with ophiolitic rocks along the eastern part of

the Izmir-Ankara-Erzincan suture zone and would not be useful in terms of geothermal resource exploration.

In Figure 1 the high amplitude total gradient seen in a curvature shape in the north well correlates with the ophiolitic rocks present in this region. It can also be suggested that from the total gradient anomalies this formation is wider beneath the thin sediment cover. It can also be suggested for the aforementioned region that these ophiolitic formations are rather thin as there is no prominent gravity anomalies.

The magnetic depth estimates from the forward modelling of magnetic spectra primarily ranged between 15 and 25 km for much of the region, showing weak correspondence of shallow depths to the bottom with some of the really large high flow and volcanic regions. No other strong geologic significance can be derived from the observed variation of the bottom depths. The magnetic depth results indicate that the magnetic part of the crust is likely to be limited to 15–25 km depth and such thinning may be caused by either a thick accumulation of non-magnetic sedimentary rocks in the subduction prism forming the present day crust or, alternatively; the deep crust is sufficiently hot in the region such that it has been demagnetized, although this heat may not have reached the surface regionally except through volcanic episodes.

Acknowledgments

We thank the General Directorate of the Mineral Research and Exploration (MTA) of Turkey for providing digital topographic, aeromagnetic and gravity data. This research was financially supported by the Cumhuriyet University, Scientific Research Projects (CUBAP) (Project code: M-281). Dhananjay Ravat extends gratitude to NASA for funding.

References

Al-Lazki, A., Seber, D., Sandvol, E., Turkelli, N., Mohamad, R., and Barazangi, M. (2003), *Tomographic Pn velocity and anisotrophy structure beneath the Anatolian Plateau (eastern Turkey) and the surrounding regions*. Geophys. Res. Lett. *30*(24), 8043.

Ates, A., Bilim, F., and Buyuksarac, A. (2005), *Curie point depth investigation of Central Anatolia, Turkey,* Pure Appl. Geophys. *162*, 357–371.

Ates, A., Kayiran, T., and Sincer, I. (2003), *Structural interpretation of the Marmara Region, NW Turkey from aeromagnetic, seismic and gravity data*, Tectonophys. *367,* 41–99.

Aydin, I., Karat, H. I., and Kocak, A. (2005), *Curie point depth map of Turkey*, Geophys. J. Int. *162*, 633–640.

Baldwin, R.T. and Langel, R. (1993), *Tables and maps of the DGRF 1985 and IGRF 1990*, Internat. Assoc. Geomagnet. Aeronomy (IAGA), Bulletin *54,* 158.

Bhattacharyya, B. K. and Leu, L. K. (1975), *Analysis of magnetic anomalies over Yellowstone National Park: mapping and Curie point isothermal surface for geothermal reconnaissance*, J. Geophys. Res. *80*, 4461–4465.

BINGOL, E. (1989), *Geological map of Turkey (Scale: 1/2.000.000)*, General Directorate of Mineral Research and Exploration (MTA), Ankara.

BLAKELY, R. J., *Potential Theory in Gravity and Magnetic Applications* (Cambridge University Press, 1995) 441 pp.

CHIOZZI, P., MATSUSHIMA, J., OKUBO, Y., PASQUALE, V., and VERDOYA, M. (2005), *Curie-point depth from spectral analysis of magnetic data in central–southern Europe*, Phys. Earth and Planet. Inter. *152*, 267–276.

CONNARD, G., COUCH, R., and GEMPERLE, M. (1983), *Analysis of aeromagnetic measurements from the Cascade Range in Central Oregon*, Geophys. *48,* 376–390.

DOLMAZ, M. N., HISARLI, Z. M., USTAOMER, T., and ORBAY, N. (2005a), *Curie-point depths based on spectrum analysis of aeromagnetic data, West Anatolian Extensional Province, Turkey*, Pure and Appl. Geophys. *162*, 571–590.

DOLMAZ, M. N., HISARLI, Z. M., USTAOMER, T., and ORBAY, N. (2005b), *Curie-point depth variations to infer thermal structure of the crust at the African-Eurasian convergence zone, SW Turkey*, Earth Planet. Spa. *57*, 373–383.

ERCAN, T., FUJITANI, T., MADSUDA, J.-I., NOTSU, K., TÖKEL, S., and TADAHIDE, U. I. (1990), *Dogu ve guneydogu Anadolu Neojen-Kuvaterner volkanitlerine iliskin yeni jeokimyasal, radyometrik ve izotopik verilerin yorumu*, Bull. of the Min. Res. Exp. (MTA) of Turkey *110*, 143–164 (in Turkish).

ERISEN, B., AKKUS, I., UYGUR, N., KOCAK, A., *Turkiye Jeothermal Envanteri (General Directorate of Mineral Research and Exploration*, MTA, Ankara 1996), pp. 480.

FINN, C. A. and RAVAT, D. (2004), *Magnetic depth estimates and their potential for constraining crustal composition and Heat flow in Antarctica*, Eos Trans. AGU, *85*(47), Fall Meet. suppl., Abstract T11A-1236.

GURBUZ, C., TURKELLI, N., BEKLER, T., GOK, R., SANDVOL, E., SEBER, D., and BARAZANGI, M. (2004), *Seismic event location calibration using the Eastern Turkey broadband seismic network: analysis of the Agri dam explosion*, Bull. Seismol. Soc. Amer. *94*(3), 1166–1171.

HAGGERTY, S. E. (1978), *The redox state of planetary basalts*, Geophys. Res. Lett. *5*, 443–446.

HESS, H, H. (1962), *History of ocean basins*. In (Eds. Engel, A.E.J., H.L. James, and B.F. Leonard), *Petrologic Studies, a Volume to Honor A. F. Buddington: Boulder, CL*, Geol. Soc. Amer. 599–620.

KESKIN, M., PEARCE, J. A., and MITCHELL, J. G. (1998), *Volcano-stratigraphy and geochemistry of collision-related volcanism on the Erzurum-Kars Plateau, North Eastern Turkey,* J. Vol. Geothermal Res. *85,* 355–404.

KESKIN, M. (2003), *Magma generation by slab steepening and breakoff beneath a subduction-accretion complex: An alternative model for collision-related volcanism in Eastern Anatolia, Turkey*, Geophys. Res. Lett. *30*(24), 8046.

KLETETSCHKA, G. and STOUT, J. H. (1998), *The origin of magnetic anomalies in lower crustal rocks, Labrador*, Geophys. Res. Lett. *25*, 199–202.

KOCYIGIT, A., YILMAZ, A., ADAMIA, S., and KULOSHVILI, S. (2001), *Neotectonics of East Anatolian Plateu (Turkey) and Lesser Caucasus: Implication for transition from thrusting to strike-slip faulting*, Geod. Acta *14*, 177–195.

LACHENBRUCH, A.H. and SASS, J.H. (1978), *Models of an extending lithosphere and heat flow in the basin and range province*. In (Smith, R. B. and Eaton, G. P. eds.), *Cenozoic Tectonics and Regional Geophysics of the Western Cordillera*, Geol. Soc. Amer. Mem. *152*, 209–250.

MCCLUSKY, S., BALASSANIAN, S., BARKA, A., DEMIR, C., ERGINTAV, S., GEORGIEV, I., GURKAN, O., HAMBURGER, M., HURST, K., KAHLE, H., KASTENS, K., KEKELIDZE, G., KING, R., KOTZEV, V., LENK, O., MAHMOUD, S., MISHIN, A., NADARIYA, M., OUZOUNIS, A., PARADISSIS, D., PETER, Y., PRILEPIN, M., REILINGER, R., SANLI, I., SEEGER, H., TEABLEB, A., TOKSÖZ, M.N., and VEIS, G. (2000), *Global Positioning system constraints on plate kinematics and dynamics in the Eastern Mediterranean and Caucasus*, J. of Geophys. Res. *105*, 5695–5719.

OKUBO, Y. and GRAF, R. J., HANSEN, R. O., OGAWA, K., and TSU, H. (1985), *Curie-point depths of the Island of Kyushu and surrounding areas, Japan*, Geophys. *50*, 481–494.

OKUBO, Y., TSU, H., and OGAWA, K. (1989), *Estimation of Curie-point temperature and geothermal structure of Island Arcs of Japan*, Tectonophys. *159*, 279–290.

Pasyanos, M.E., William, R.W, Flanagan, M.P., Goldstein, P., and Bhattacharyya, J. (2004), *Building and testing an 'a priori' geophysical model for Western Eurasia and North Africa*, Pure Appl. Geophys. *161*, 235–281.

Pearce, J. A., Bender, J. F., De Long, S. E., Kidd, W. S. F., Low, P. J., Guner, Y., Saroglu, F., Yilmaz, Y., Moorbath, S., and Mitchell, J. G. (1990), *Genesis of collision volcanism in Eastern Anatolia, Turkey*, J. Vol. Geotherm. Res. *44*, 189–229.

Pollack, H. N., Hurter, S.J., and Johnson, J.R. (1993), *Heat flow from the Earth's interior: Analysis of the global data set*, Rev. of Geophys. *31*(3), 267–280.

Ravat, D. (2004), *Constructing full spectrum potential–field anomalies for enhanced geodynamical analysis through integration of surveys from different platforms (INVITED)*, Eos Trans. AGU, *85*(47), Fall Meet. suppl., Abstract 644A-03.

Ravat, D., Pignatelli, A., Nicolosi, I., and Chiappini, M. (2005), *Comparison of methods of mapping the depth to the top and the bottom of magnetic sources using layered and random synthetic magnetic models*, EOS Trans. AGU *86*(18), Joint Assembly Suppl., Abstract Book, Washington, USA.

Roest, W. R., Verhoef, J., and Pilkington, M. (1992), *Magnetic interpretation using the 3-D analytic signal*, Geophys. *57*(1), 116–125.

Ross, H. E., Blakely, R. J., and Zoback, M. D. (2004), *Testing the utilization of aeromagnetic data for the determination of Curie-isoterm depth*, Eos Trans. AGU, *85*(47), Fall meet. suppl., Abstract T31A-1287.

Roy, R. F., Blackwell, D. D., and Birch, F. (1968), *Heat generation of plutonic rocks and continental heat flow provinces*, Earth and Planet. Sci. Lett. *5*, 1–12.

Shuey, R.T., Schellinger, D.K., Tripp, A.C., and Alley, L.B. (1977), *Curie depth determination from aeromagnetic spectra,* Geophys. J. of the Royal Astron. Soc. *50*, 75–101.

Spector, A. and Grant, F. S. (1970), *Statistical models for interpretation aeromagnetic data*, Geophys. *35*, 293–302.

Storetvedt, K. M., *Global Wrench Tectonics* (Fagbokforlaget, Norway 2003), pp. 397.

Tanaka, A., Okubo, Y., and Matsubayashi, O. (1999), *Curie-point depth based on spectrum analysis of the magnetic anomaly data in East and Southeast Asia*, Tectonophys. *306*, 461–470.

Tezcan, A. K., *Geothermal studies, their present status and contribution to heat flow contouring in Turkey in terrestrial heat flow in Europe* (*eds. Cermak, V., Rybach, L.*) (Springer Verlag, Berlin, 1979), pp. 283–291.

Tezcan, A. K. and Turgay, M. I. (1987), *Heat flow density distribution in Turkey,* General Directorate of Mineral Research and Exploration (MTA), Ankara.

Tezcan, A. K. and Turgay, M. I. (1989), *Turkiye ısı akısıs haritası*. General Directorate of Mineral Research and Exploration (MTA), Ankara.

Turkelli, N., Sandvol, E., Zor, E., Gok, R., Bekler, T., Al-Lazki, A., Karabulut, H., Kuleli, S., Eken, T., Gurbuz, C., Bayraktutan, S., Seber, D., and Barazangi, M. (2003), *Seismogenic zones in Eastern Turkey*, Geophys. Res. Lett. *30*(24), 8039.

Zor, E., Sandvol, E., Gurbuz, C., Turkelli, N., Seber, D., and Barazangi, M. (2003), *The Crustal structure of the East Anatolian Plateau (Turkey) from receiver functions*, Geophys. Res. Lett. *30* (24), 8044.

(Received April 14, 2006, accepted November 7, 2006)
Published Online First: April 23, 2007